Identification of Key circRNAs/lncRNAs/miRNAs/ mRNAs and Pathways in Preeclampsia Using Bioinformatics Analysis

Authors' Contribution:
Study Design A
Data Collection B
Statistical Analysis C
Data Interpretation D
Manuscript Preparation E
Literature Search F
Funds Collection G

ABCDEF 1 **Siwei Liu**
BCDF 2 **Xie Xie**
BCF 1 **Huajiang Lei**
BC 1 **Bingyu Zou**
AG 1 **Lan Xie**

1 Department of Obstetrics and Gynecology, Sichuan Academy of Medical Sciences and Sichuan Provincial People's Hospital, Chengdu, Sichuan, P.R. China
2 Department of Obstetrics and Gynecology, Sichuan Academy of Medical Sciences and Sichuan Provincial People's Hospital, School of Medicine, University of Electronic Science and Technology of China, Chengdu, Sichuan, P.R. China

Corresponding Author: Lan Xie, e-mail: chocharlotte@163.com
Source of support: This work was supported by Sichuan Science and Technology Support Plan Project (No. 2015SZ0165) and the Science and Technology Project of Sichuan Health and Family Planning Commission (No. 150237)

Background: This study aimed to identify significantly altered circRNAs/lncRNAs/miRNAs/mRNAs pathways in preeclampsia (PE), investigate their target relationships, and determine their biological functions.

Material/Methods: Base on RNA-seq technique and the GEO database, expression profiles of circRNAs/lncRNAs/miRNAs/mRNAs related to PE were obtained. Differentially expressed RNAs were determined using the Limma package in R. Gene set enrichment analysis (GSEA) was performed using GSEA software (v. 3.0) and illustrated by ClusterProfiler and ggplot2 package in R. DAVID database (v. 6.8) was implemented to analyze functional categories and the association between genes and the corresponding Gene Ontology (GO) classification. The R visualization package GOPlot was used to get a better visualization of the relationships between genes and the selected functional categories. CeRNA networks which visualized the correlations between circRNA/lncRNA-miRNA-mRNA were constructed using Cytoscape software (v. 3.6.0). Targetscan and miRanda database were used to predict target relationships between circRNA/lncRNA-miRNA-mRNA. QRT-PCR and luciferase reporter assay were used to verify the expression and target relationship of has_circ_0088196/LINC01492/miR-100-5p/LIF (leukemia inhibitory factor).

Results: The jak-stat signaling pathway was activated and miR-100-5p was downregulated in PE compared with normal tissues both in collected placental tissue samples and GEO database. Upregulated LIF, LINC01492, and hsa_circ_0088196 were negatively correlated with miR-100-5p expression and had a targeted relationship with miR-100-5p.

Conclusions: miR-100-5p may suppress PE development, while LIF, LINC01492, and hsa_circ_0088196 may promote it though inhibiting miR-100-5p. The jak-stat signaling pathway was activated and involved in PE progression.

MeSH Keywords: MicroRNAs • Pre-Eclampsia • RNA, Long Noncoding • Pre-Eclampsia

Full-text PDF: https://www.medscimonit.com/abstract/index/idArt/912801

📄 3881   ▦ 1   📊 7   📚 39

Background

Preeclampsia (PE) is a pregnancy-related syndrome characterized by high blood pressure and proteinuria, leading to a variety of pathophysiological processes, including endothelial dysfunction, systemic inflammation, and impaired implantation [1]. PE is one of the main reasons for maternal, fetal, and neonatal morbidity and mortality as it may cause iatrogenic preterm birth, intrauterine growth restriction, and has a high risk of placental abruption [2]. After 20 weeks of gestation, PE, which can be classified by early onset PE (EOPE, 34 weeks) and late onset PE (LOPE), may develop at any time [3]. There are 2 theories to explain the occurrence of PE, one is the hypoxia ischemia of the placenta, and another is the immunology of PE [4]. Despite a lot of research on this topic, the cause of PE is still elusive [5].

Gene set enrichment analysis (GSEA) is a popular calculation method for identification of differentially expressed genes and microRNAs (miRNAs) with certain characteristics [1,6]. It has also been applied to analyze the slight changes in the expressions of genes that belong to a key pathway [7]. A good example of the application of GSEA was the experiment of drug response in cancer cell lines conducted by Alain et al. that compared each of the standard gene set collections in the context of a large dataset of drug response in human cancer cell lines and found that the GSEA results varied significantly [8]. KEGG has been used to try to connect higher order functional information with genomic information [9]. It has been successfully applied to analyze the genes and pathways in human diseases. For instance, Erik et al. evaluated the gene expression profile of biopsy tissue obtained from the neck of human abdominal aortic aneurysm, and revealed marked pathways [10].

Leukemia inhibitory factor (LIF) is involved in cell differentiation induction and mesenchymal to epithelial conversion, and may also have a role in immune tolerance at the maternal-fetal interface. LIF has been recently identified as a potential biomarker for several diseases. It has been reported to negatively regulate tumor-suppressor p53 through Stat3/ID1/MDM2 in colorectal cancers [11], and also LIF withdrawal is reported to activate mTOR signaling pathway in mouse embryonic stem cells through the MEK/ERK/TSC2 pathway [12]. Importantly, some studies found that LIF was high expression in preeclamptic patients [13–15]. One study reported that LIF could regulate chondroitin sulfate proteoglycan 4 (CSPG4) expression to impact human trophoblast function [16]. However, factors influencing the role of LIF in PE are unclear.

According to previous studies, miRNAs play crucial roles in PE. In the placenta, miR-141 was among the top abundant miRNAs with high levels in plasma during pregnancy [17]. Lately, miR-141 was found to play a crucial role in the intercellular communication between fetal trophoblast and maternal immune cells, and it could be used as a potential pregnancy biomarker to indicate disease such as PE [18]. Orsolya et al. found that miR-210, one of the most common PE-related differentially expressed miRNAs, was highly expressed in both placenta and circulation of PE patients, and its interaction with mRNA contributed to the pathogenesis of PE [19].

Cyclic RNA is a peculiar type of non-coding RNA interacting closely with miRNA in mammalian cells, with unique circular framework [20]. Researchers attempted to explore the potential roles of dysregulated circRNAs in the pathological genesis of PE. From a total of 22796 circRNAs, Bai et al. identified 300 differentially expressed circRNAs and found the potential non-invasive biomarker hsa_circ_0007121 which could help to predict PE [2]. In study conducted by Zhang et al., circRNA expressions in PE placentas and healthy samples were measured, and the result suggested that the detection of the circRNAs could make great contribution to the prediction of PE [21].

Long non-coding RNAs (lncRNAs) are a type of universal genes with multiple biological functions [22]. He et al. identified that lncRNA MALAT-1 was downregulated in the PE patients, and suggested that the silencing of MALAT-1 suppressed proliferation, led G_0/G_1 arrest, expedited apoptosis, and restrained migration and invasion of JEG-3 cells [23]. A microarray study conducted by He et al. identified 738 differentially expressed lncRNAs in PE patients compared to normal samples, and 3 of them (LOC391533, LOC284100, and CEACAMP8) were approved to be upregulated in PE placentas and related to lipid metabolism and angiogenesis [24].

In our study, we preformed GSEA to identify activated jak-stat signaling pathway and found that miR-100-5p had low expression in the placenta samples from PE patients. Thus, LIF was considered a potential mRNA related to PE. Moreover, LIF had a negative correlation with miR-100-5p expression, and there was a targeting relationship between them. Additionally, we identified closely associated circRNA and lncRNA. Our findings suggested that LINC01492 and hsa_circ_0088196, which inversely associated with miR-100-5p, were highly expressed in PE. Encouragingly, we found that the circRNA and lncRNA had targeting relationships with miR-100-5p.

Material and Methods

Tissue samples and serum samples

A total of 13 placental tissue samples from PE patients and paired placental tissues samples from 3 age- and gender-matched healthy people were obtained from Sichuan Academy of Medical Sciences and Sichuan Provincial People's Hospital

between 2015 and 2016. The fresh specimens were stored at –80°C liquid nitrogen until further use. All included patients provided written, informed consent. The Human Research Ethics Committee of Sichuan Academy of Medical Sciences and Sichuan Provincial People's Hospital approved the study.

RNA extraction and microarray experiments

Total RNA was isolated from 3 randomly selected paired of placental tissue samples from collected 13 paired tissues by using RecoverAll™ Total Nucleic Acid Isolation Kit (Life Technologies, USA) and analyzed by RiboBio (Guangzhou, China) for miRNA microarray analysis. Gene expression was profiled with Illumina microarrays, which were scanned with BeadArray Reader (Illumina, USA). The raw data was obtained by GenomeStudio (Illumina, USA) and normalized using the WateRmelon package. The differential expressions of genes were assessed by a modified t-test (Limma package, Bioconductor).

Microarray analysis

The raw data of circRNAs, lncRNAs, mRNAs, and miRNAs expressions in PE tissue and normal tissues were downloaded on GEO (*https://www.ncbi.nlm.nih.gov/geo/*) (GSE96985, including GSE96983 and GSE96984). Each of them contained 7 placental samples with 3 PE patients and 4 normal female patients, focusing on basal plates of placenta. Processing of gene expression data was carried out using the Limma package in the R software. Data in each array was normalized using quantile normalization procedure. Genes that were differently expressed between normal and PE tissue were identified by t-test in the R package Limma [25]. We applied t-test in order to filter the differentially expressed lncRNAs, circRNAs miRNAs and lncRNAs in PE. RNAs in GSE96985 were considered as significantly different if they meet the conditions of P value <0.05 (BH method) and $|\log_2 FC| >1$. As for the differentially expressed miRNAs in RNA-seq of tissues, the $|\log_2 FC|$ threshold was set to be 0.5 and P value (BH method) was less than 0.05.

Gene set enrichment analysis (GSEA)

In order to identify pathways of intersecting genes, KEGG enrichment analysis was implemented. The genes identified by microarray analysis were submitted to GSEA V3.0, using the local human-KEGG database and $\log_2$ ratio of classes method. KEGG pathways in PE and normal tissue with significant enrichment results were demonstrated on the basis of NES (Net enrichment score), gene ratio and P value. Ggplot2, ClusterProfiler, DOSE and ggjoy R packages were applied to visualize the results, which presented the dysfunctional pathways in PE compared with normal tissue.

Gene Ontology (GO) classification analysis

We applied Gene Ontology (GO) classification, including GO-BP (biological process), GO-MF (molecular function), and GO-CC (cellular component), to uncover the functions of intersecting genes and further test the biological links in co-regulated genes. DAVID V6.8 (*http://david.ncifcrf.gov*), a web-based bioinformatics resource intended for functional genomics analysis, was used to implement annotation and visualization. We submitted the gene list consisting of 117 differentially expressed mRNAs screened under conditions of $|\log_2 FC| >2.6$ and P value <0.0005 to the DAVID database, using the official gene symbol method. Five GO terms with significant P value was selected according to the BP, CC, and MF results, respectively. R package GOplot was used to integrate the quantitative information by implementing novel and high-quality plotting. This provided us with a collection of multilayered and pre-specified charts. Valuable information was added to each layer to display the intended message.

CeRNA network

Pearson correlation coefficient (PCC) functioned as a measurement of linear relationship between fixed-range variables. The greater the absolute value of the correlation coefficient, the stronger the correlation was between 2 variables. PCC that was greater than zero represented a positive correlation, while PCC less than zero indicated a negative correlation. In order to identify the potential target relationship of differentially expressed RNAs in PE, networks of circRNAs – miRNAs – mRNAs, and lncRNAs – miRNAs – mRNAs were constructed on the basis of PCC. Four common disordered miRNAs in the GSE96985 dataset and our RNA-seq dataset were chosen as the starting points of the network. According to references [26], 0.7 indicates a moderately negative (positive) correlation. The cutoffs for PCC between lncRNA/circRNA – miRNA – mRNA was thus set as 0.7 with a P value <0.05. The RNAs satisfying these cutoff conditions were preserved as nodes in the network, and the value of PCC represented the relationship between these nodes. R package psych was used to generate node data and edge data, which were the 2 necessary data sets required by Cytoscape (v. 3.6.0) to visualize the network results.

Integrated analysis of miRNA targets

MiRNAs that were targeted by the lncRNAs in the network were predicted by using the TargetScan database version 6.0 (*http://www.targetscan.org/*) and miRanda (*http://www.microrna.org/microrna/home.do*). We further combined the analysis of differentially expressed miRNAs with the target prediction of miRNAs. The intersecting gene set was subject to in-depth analysis.

Table 1. Primer sequences used for qRT-PCR.

Genes	Primer sequences
LIF	F: 5'-TGAACCAGATCAGGAGCCAA-3'
LIF	R: 5'-TCGGTTCACAGCACACTTCA-3'
U6	F: 5'-CTCGCTTCGGCAGCACA-3'
U6	R: 5'-AACGCTTCACGAATTTGCGT-3'
MiR-100-5p	F: 5'-AAGAGAACCCGTAGATCCG-3'
MiR-100-5p	R: 5'-CTCAACTGGTGTCGTGGA-3'
has_circ_0088196	F: 5'-GCCATGAAGGGCTTTGAGGA-3'
has_circ_0088196	R: 5'-GCCATGAAGGGCTTTGAGGA-3'
GAPDH	F: 5'-TCGGAGTCAACGGATTTGGT-3'
GAPDH	R: 5'-TTCCCGTTCTCAGCCTTGAC-3'

F – forward primer; R – reverse primer.

Quantitative real time polymerase chain reaction (qRT-PCR)

Total RNA was isolated and reverse-transcribed into complementary DNA (cDNA) before qRT-PCR analysis. U6 and reduced glyceraldehyde-phosphate dehydrogenase (GAPDH) expressions served as controls. The expression of hsa_circ_0088196, LIF, miR-100-5p, and LINC01492 was quantified using the $2^{(-\Delta\Delta Ct)}$ method. The primers we used are listed in Table 1.

Luciferase reporter assay

HEK293T cells at the confluency of 5×10^4 cells per well were placed in a 24-well plate. The fragments of LIF 3'-UTR, LINC01492, and hsa_circ_0088196 with both wildtype and mutant binding sites by miR-100-5p, on each side with enzyme cleavage sites, were synthesized and subcloned into pmirGLO luciferase reporter vectors (Promega). After incubating overnight, the cells were transfected with constructed vector (10 ng), along with negative control mimics (50 ng) or miR-100-5p mimic (50 ng) by using Lipofectamine 2000 (ThermoFisher) using the protocols of the manufacturer. The transfected cells were collected after 48 hours. Dual Luciferase reporter assay kit (Promega) was utilized for luciferase activity analysis and the luciferase activity was detected through SpectraMax L (Molecular Devices, CA, USA).

Results

MiR-500-5p had low expression in PE

Microarray analysis generated 7008 differentially expressed circRNAs, 1789 differentially expressed lncRNAs, 46 differentially expressed miRNAs (Figure 1A), and 1950 differentially expressed mRNAs in PE based on the GSE96983 dataset (P<0.05 and |log$_2$FC| >1). Differentially expressed miRNAs in our RNA-seq PE tissues were identified if P was <0.05 and |log$_2$FC| was >0.5. In our PE tissue samples, 33 differentially expressed miRNAs were identified (Figure 1B). There were 4 common differentially expressed miRNAs shared by GSE96983 and patient placental tissues (Figure 1C). The top 30 differentially expressed mRNAs (15 upregulated and 15 downregulated), the circRNAs, and the lncRNAs were respectively demonstrated by heatmapping (Figure 1D–1F). MiR-100-5p had low expression in PE tissues in the GSE96983 dataset and consistently showed low expression in tissue RNA-seq (Figure 1A, 1B). LIF, hsa_circ_0088196, and LINC01492 were upregulated in PE tissue samples (Figure 1D–1F).

GO terms enrichment analysis results

DAVID database analyzed the gene list consisting of 117 differentially expressed mRNAs which were screened out under condition of |log$_2$FC| >2.6 and P value <0.0005. Five most significantly enriched BP, CC, and MF terms were presented in the bar graph. Negative regulation of cell proliferation (GO: 0008285) in BP demonstrated the lowest P value, and z-score marked it as a decreasing GO term (Figure 2A). P value of extracellular space (GO: 0005615) was lowest in CC and it was an increasing GO term according to the z-score (Figure 2A). Calcium ion binding (GO: 0005509) exhibited the lowest P value and was a decreasing GO term in MF (Figure 2A). In Figure 2B, a z-score was assigned to the x-axis and a negative log P value was assigned to the y-axis, and the area of displayed bubbles was in direct proportion to the number of genes in a certain GO term. The 3 different colors in the GOBubble graph corresponded to the 3 major categories (BP, CC, and MF), and a bubble dot stood for a GO term (Figure 2B). Negative regulation of cell proliferation (GO: 0008285) had the largest number of genes determined by the area of this bubble and its P value was the highest in BP, while the extracellular space (GO: 0005615) GO term had the highest P value and contained the largest number of genes in CC (Figure 2B). The GOCircle in Figure 2C shows the overview of the most important terms. The outer circle is a scatter plot for each GO term with logFC assigned to genes, with the red dot representing upregulated genes and the blue dots representing downregulated genes (Figure 2C). Extracellular exosome (GO: 0005615) had the largest number of genes upregulated and the z-score indicated it was an increasing GO term (Figure 2C). The left side of the GOChord displayed whether the gene was upregulated or downregulated, and the right side represented different GO terms (Figure 2D). The linked band indicated that a gene was in a certain GO term (Figure 2D). *SERPINA* had the highest logFC while *OR1J4* exhibited the lowest logFC (Figure 2D).
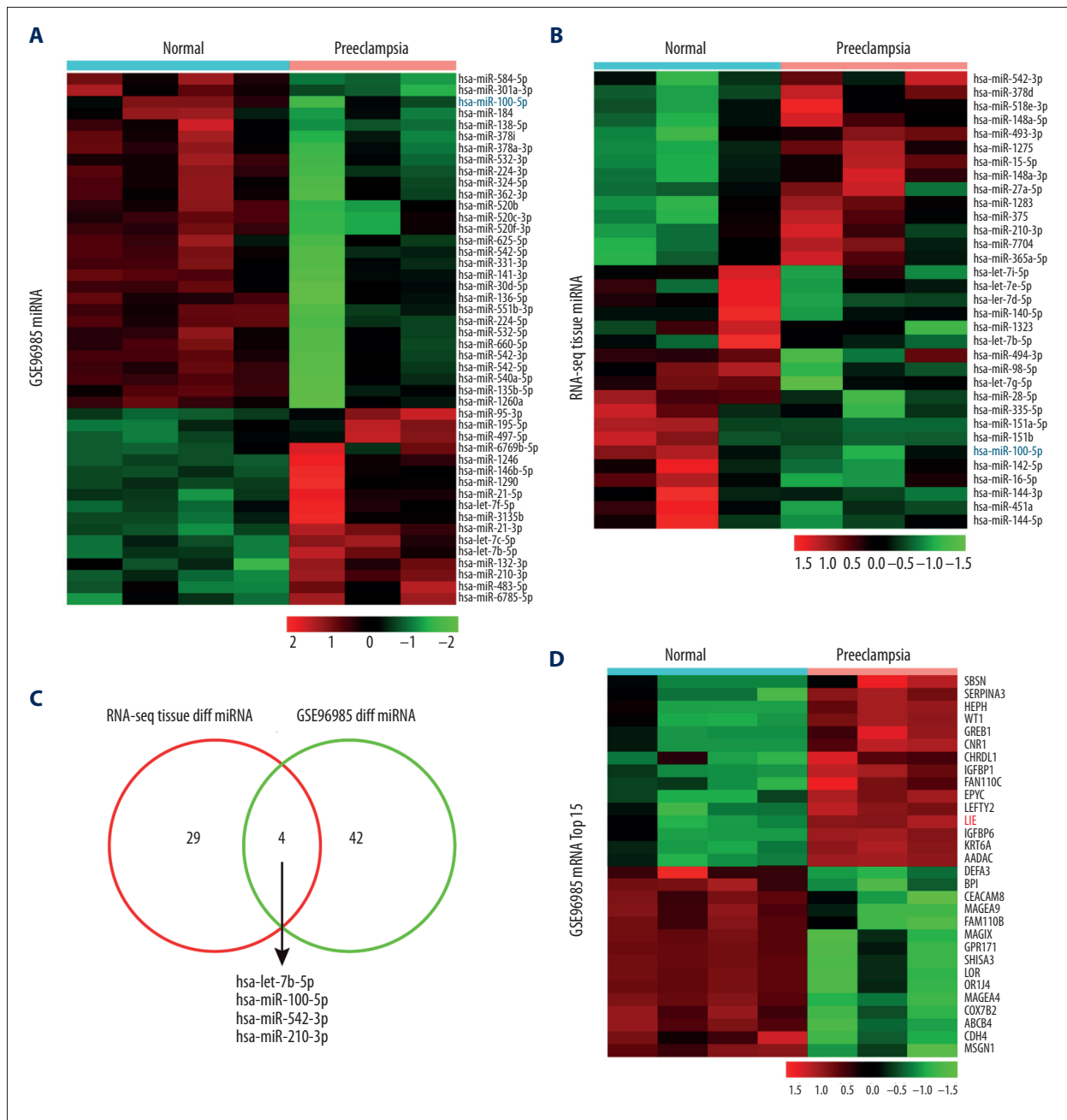
Hierarchical clustering results of gene expression and functional categories

GOCluster plot displayed a circular dendrogram of clustered expression profiles. The outer ring represented the assigned GO terms, the middle ring indicated the color-coded logFC of the genes, and the inner ring represented genes assigned to the GO terms (Figure 3A, 3B). The figure was clustered together base on logFC value (Figure 3A) and others were clustered together on the basis of their corresponding functional categories (Figure 3B). The GO term extracellular region had a large number of grouped genes with high fold change, while all the significantly downregulated genes were involved in the extracellular region (Figure 3A, 3B).

The jak-stat signaling pathway was activated in PE

Jak-stat signaling pathway was illustrated as an activated pathway in PE tissue by dot plot based on the GSEA results, with the P value scale demonstrated by color intensity (Figure 3C). Around 50 genes, with 34% of genes differentially expressed, were included in jak-stat signaling pathway according to its
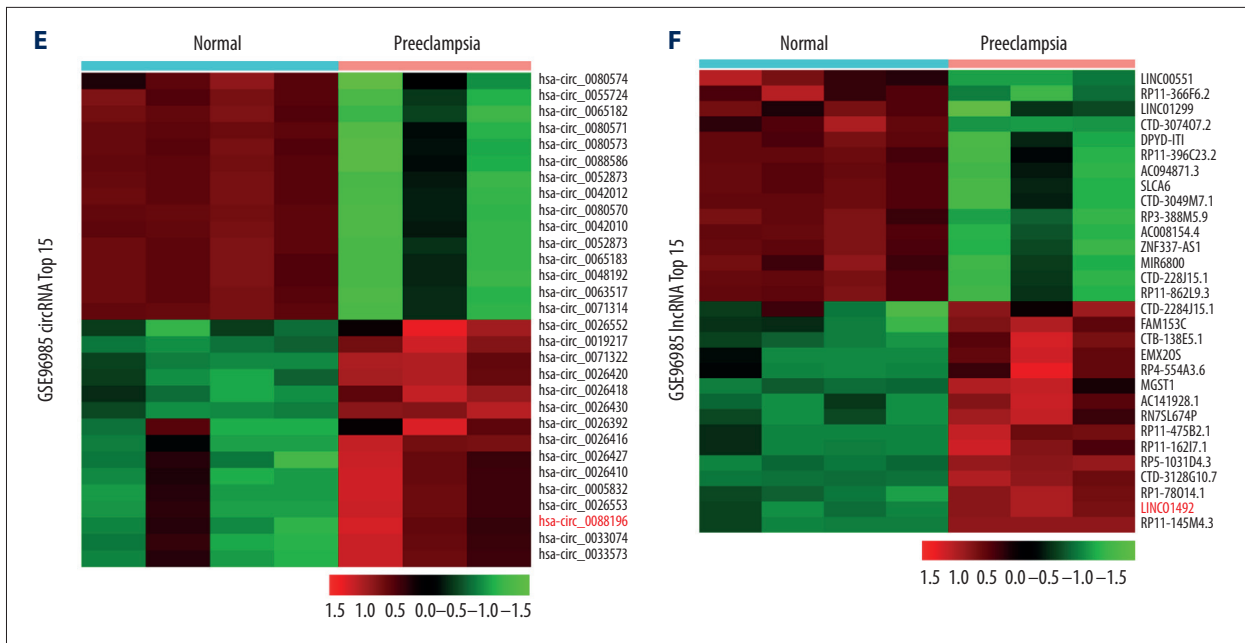
This work is licensed under Creative Common Attribution-NonCommercial-NoDerivatives 4.0 International (CC BY-NC-ND 4.0)

1683

Indexed in: [Current Contents/Clinical Medicine] [SCI Expanded] [ISI Alerting System] [ISI Journals Master List] [Index Medicus/MEDLINE] [EMBASE/Excerpta Medica] [Chemical Abstracts/CAS]

Figure 1. MiR-100-5p had low expression in preeclampsia (PE) tissue. (**A**) Heatmap of the top 20 differentially expressed miRNAs from the GEO microarray GSE96985: miR-100-5p was downregulated in PE tissue ($|\log_2 FC| > 1$, adjusted $P < 0.05$). (**B**) Heatmap of differentially expressed miRNAs from placental tissue RNA-seq: miR-100-5p was downregulated in PE ($|\log_2 FC| > 0.5$, adjusted $P < 0.05$). (**C**) The intersection of differentially expressed miRNAs of GSE96985 and differentially expressed miRNAs of placental tissue RNA-seq, in which 4 miRNAs were included. (**D**) Heatmap of the top 30 differentially expressed mRNAs ($|\log_2 FC| > 1$, adjusted $P < 0.05$). (**E**) Heatmap view of the top 30 differentially expressed circRNAs with 15 upregulated and 15 downregulated in PE tissues ($|\log_2 FC| > 1$, adjusted $P < 0.05$). (**F**) Heatmap of the top 30 differentially expressed lncRNAs ($|\log_2 FC| > 1$, adjusted $P < 0.05$).
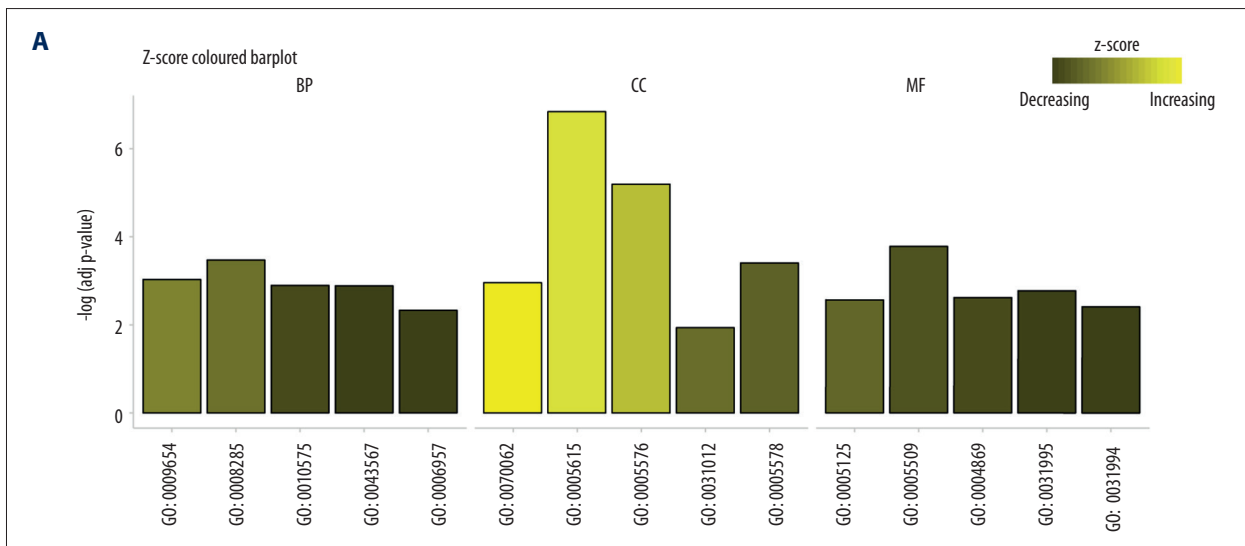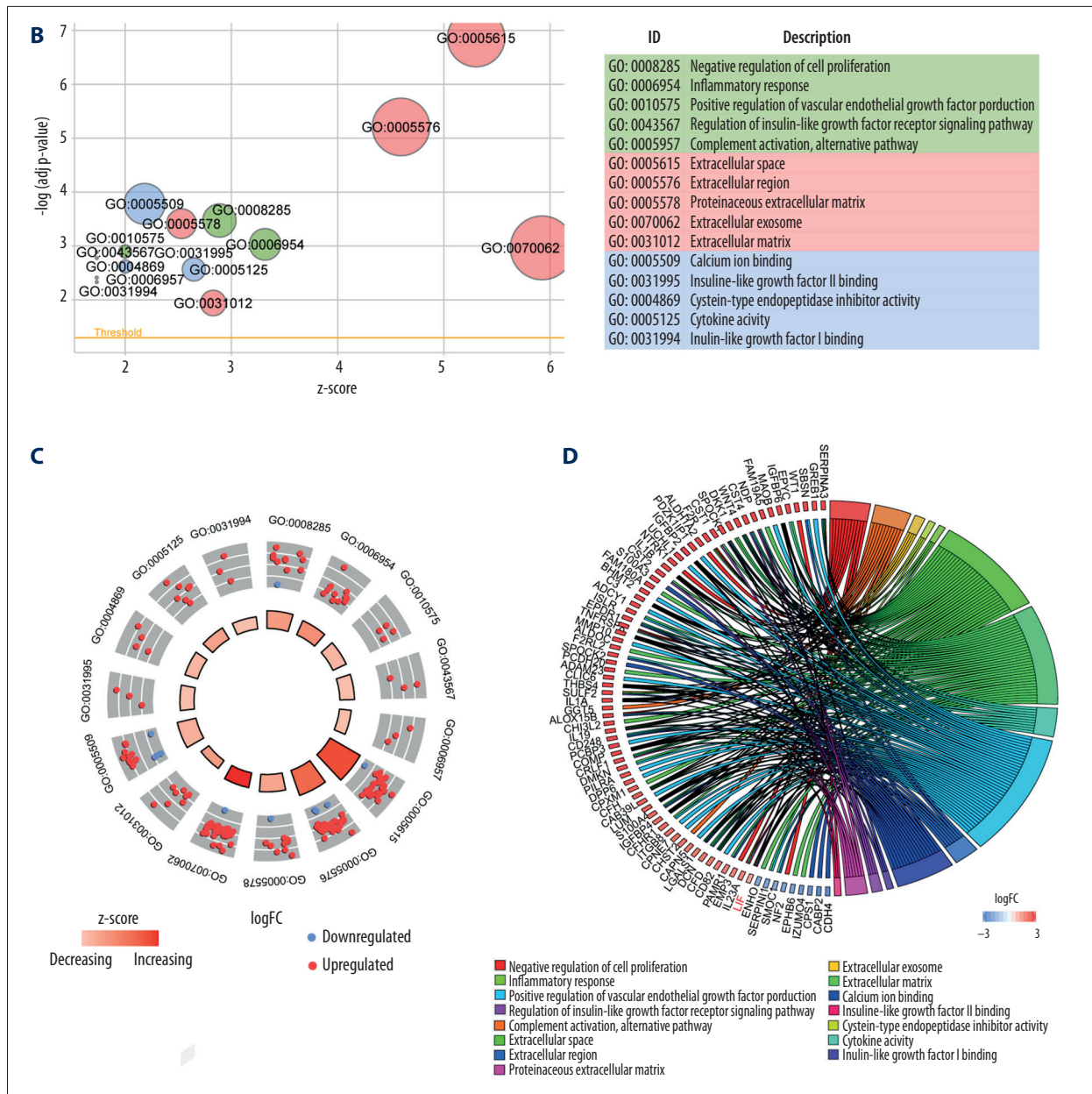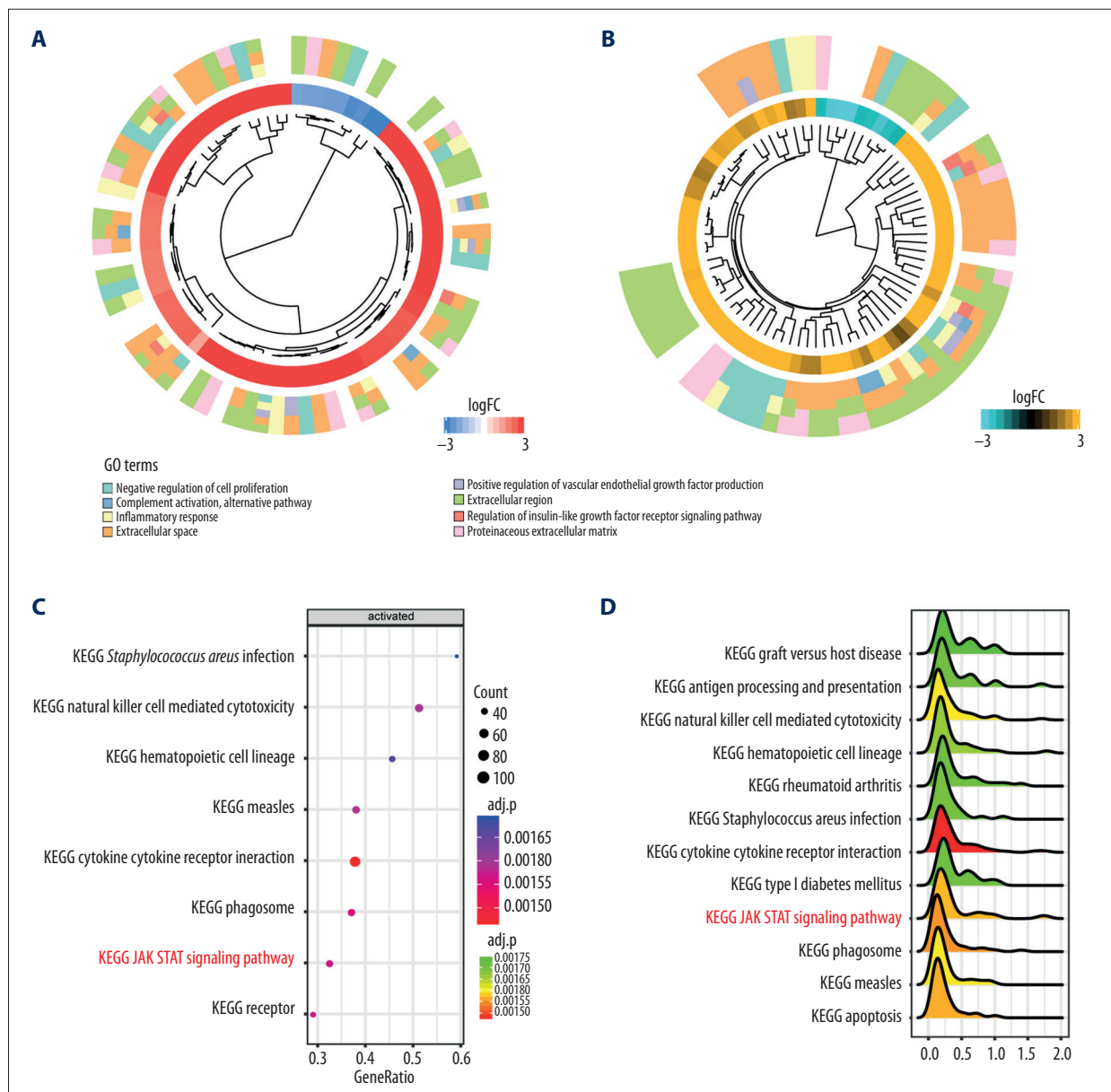
Figure 2. GO (Gene Ontology) terms enrichment analysis results. (**A**) Z-score colored bar plot of GO terms. GO ID was assigned to x-axis and negative log *P* value was assigned to y-axis. The color intensity represented the value of z-score. Higher z-score indicated the GO term as an increasing term while lower z-score indicated it as a decreasing GO term. The decreased negative regulation of cell proliferation, the increased extracellular space and the decreased calcium ion binding had the lowest adjust *P* value among biological process (BP), cellular component (CC) and molecular function (MF) respectively. (**B**) Bubble plot of GO terms. Z-score was assigned to x-axis and negative log *P* value was assigned to the y-axis. Bubble area was positively proportional to the number of genes in a certain GO term. Extracellular space had the largest amounts of genes and the lowest *P* value. (**C**) GOCircle plot; the inner ring was a bar plot where the bar height indicated the significance of the term (-log10 *P* value) and the color indicated the z-score. The outer ring displayed scatterplots of the expression levels (logFC) for the genes in each term. The increased extracellular exosome had the largest number of genes upregulated. The decreased calcium ion binding had the largest number of downregulated genes. (**D**) GOChord plot of the relationship between the list of selected genes and their corresponding GO terms, together with the logFC of the genes. Left half of GOChord displayed whether the gene was up- or down-expression. The right half represented different GO terms with different colors. A gene was linked to a certain GO term by the colored bands. *SERPINA* had the highest logFC while *OR1J4* exhibited the lowest logFC.

gene ratio and the dot size (Figure 3C). Ridge plot also indicated the activation of the jak-stat signaling pathway (Figure 3D). GSEA plot confirmed that the majority of differentially expressed genes involved in the jak-stat signaling pathway were upregulated as the running enrichment score was positive for most of them (Figure 3E). Seven enriched KEGG pathways that were significantly dysregulated were ranked according to the NES value (Figure 3F). The jak-stat signaling pathway was the most upregulated pathway among them in PE tissue, and more than 200 genes in this pathway were upregulated (Figure 3F).

The relationship of mRNA LIF, miR-100-5p LINC01492, and has-circ_0088196

The ceRNA networks of lncRNAs – miRNAs – mRNAs network and circRNAs – miRNAs – mRNAs networks were visualized by Cytoscape (V 3.6.0) (Figure 4A, 4B). In both networks, we chose mRNA LIF as an interesting mRNA which was upregulated and also one of the upstream genes in jak-stat signaling pathway. In addition, miR-100-5p was the only intersection of 2 ceRNA networks: miRNAs targeted LIF and miRNAs that had correlation of expression with LIF (Figure 4C, 4D). The intersection of LINC01492 targeted miRNAs and miRNAs that had correlation with LINC01492 included let-7b-5p and miR-100-5p, and so was the intersection of hsa_circ_0088196 targeted miRNAs and miRNAs that had
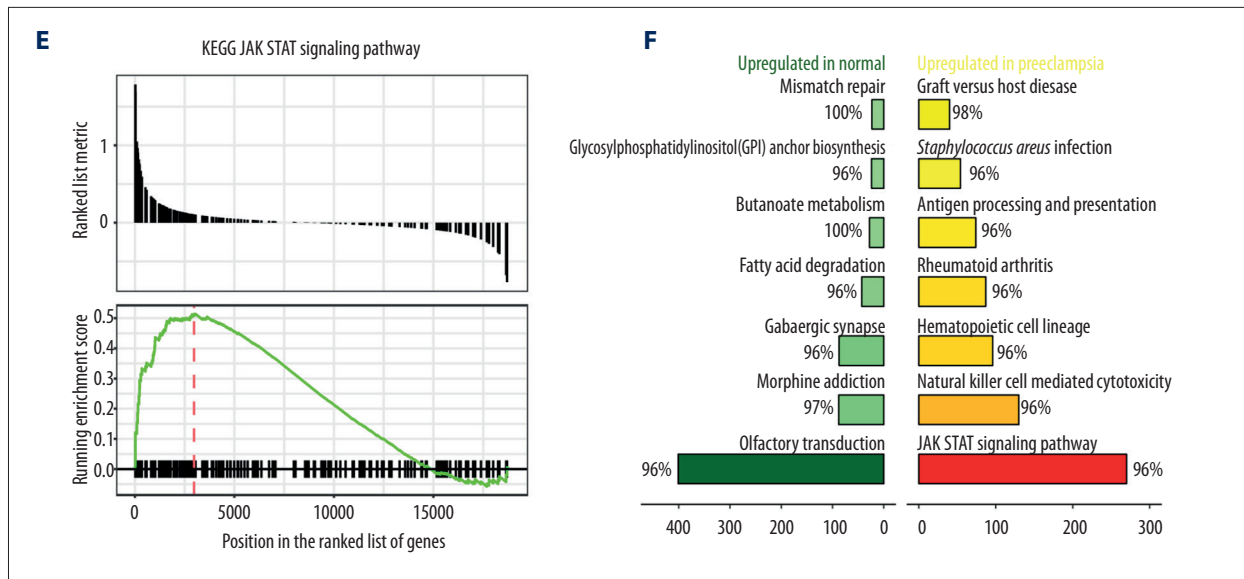
This work is licensed under Creative Common Attribution-NonCommercial-NoDerivatives 4.0 International (CC BY-NC-ND 4.0)

1686

Indexed in: [Current Contents/Clinical Medicine] [SCI Expanded] [ISI Alerting System]
[ISI Journals Master List] [Index Medicus/MEDLINE] [EMBASE/Excerpta Medica]
[Chemical Abstracts/CAS]

Figure 3. Hierarchical clustering results of gene expression and functional categories and GSEA results. (**A**) GOCluster of genes grouped by their expression level. GO terms, logFC value and related genes were assigned from the outer circle to the inner circle. Clusters in GOCluster were likely to contain sets of co-regulated genes. (**B**) GOCluster of genes grouped by their functional categories. Extracellular region had large amounts of grouped genes with high fold change, while all the significantly downregulated genes were involved in extracellular region. (**C**) Dot plot of dysregulated pathways in PE tissue. The jak-stat signaling pathway was activated. The color intensity of the nodes displayed the enrichment degree of KEGG pathways. Gene ratio was assigned to horizontal axis as the proportion of differential genes in the whole gene set. The dot size represented the gene counts in a certain pathway. (**D**) Ridge plot of dysregulated pathways in PE tissue. Joy plot indicated that jak-stat signaling pathway was activated. Color intensity of the peaks represented enrichment significance. *P* value was assigned to the horizontal axis. (**E**) GSEA plot of genes involved in jak-stat signaling pathway in PE tissue. Running enrichment score was negative for most differentially expressed genes. (**F**) Ranking plot of seven enriched KEGG pathways arranged according to the NES. The jak-stat signaling pathway was the most upregulated pathway in PE tissue among 7 pathways.

correlation with hsa_circ_0088196 (Figure 4E, 4F). As a result, LIF, miR-100-5p, LINC01492, and hsa_circ_0088196 were chosen for further investigation of expression level.

The expression levels of LIF, miR-100-5p, LINC01492, and hsa_circ_0088196 in PE tissue

Ten placental tissues samples from PE patients and paired placental tissues samples from 10 age- and gender-matched healthy people were obtained and RNAs were extracted for investigation of expression. LIF, LINC01492, and hsa_circ_0088196 were upregulated in PE group compared to normal group, while miR-100-5p was downregulated in PE (Figure 5A–5D), and the result confirmed the results of microarray analysis. In addition, the correlations of the expression levels were examined. MiR-100-5p was validated to be negatively correlated with LIF, LINC01492, and hsa_circ_0088196 (Figure 6A–6C), whereas hsa_circ_0088196 and LINC01492 were both positively correlated with LIF (Figure 6D, 6E). A table illustrating the expression level correlation of the four RNAs was placed, in which 1 indicates the same molecule, + indicates positive correlation and – indicates negative correlation (Figure 6F).

Targeting relationship verified by luciferase report assay

Although the expression correlations of the RNAs indicated potential ceRNAs network of them, targeting verification was conducted to further learn about their relationships. In luciferase reporter assay, the binding of miRNAs on the targeting sites could reduce the luciferase expression. The wildtype targeting sequences groups of LIF 3'UTR, LINC01492, and hsa_circ_0088196 co-transfected with miR-100-5p demonstrated decreased luciferase activity compared to mutant sequences groups and miR-NC groups, indicating that miR-100-5p targeted LIF and was targeted by LINC01492 and hsa_circ_0088196 (Figure 7A–7F).

Discussion

From this research, we conducted the GO analysis for PE base on DAVID database and visualized by GOplot package. According to the z-score colored bar plot, with significant *P* value, Negative regulation of cell proliferation (GO: 0008285) in BP and calcium ion binding (GO: 0005509) in MF were downregulated while
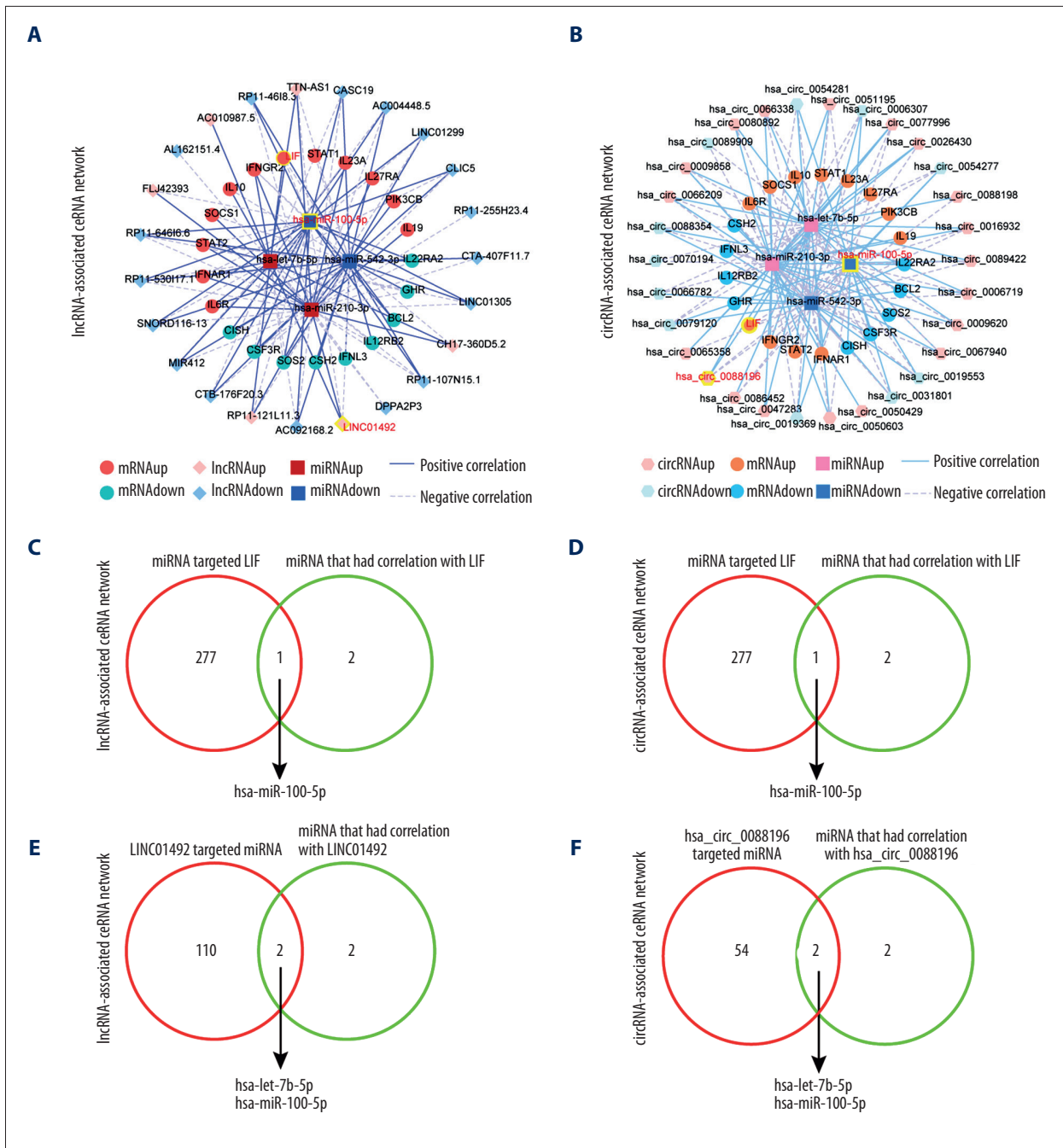
Figure 4. lncRNA/circRNA – miRNA – mRNA ceRNA network. (**A**) Network of lncRNAs – miRNAs – mRNAs. (**B**) Network of circRNAs – miRNAs – mRNAs. (**C**) Venn diagram of miRNA targeted LIF and miRNA that had correlation with LIF in lncRNA-associated ceRNA network. (**D**) Venn diagram of miRNA targeted LIF and miRNA that had correlation with LIF in circRNA-associated ceRNA network. (**E**) Venn diagram of LINC01492 targeted miRNA and miRNA that had correlation with LINC01492 in lncRNA-associated ceRNA network. (**F**) Venn diagram of hsa_circ_0088196 targeted miRNA and miRNA that had correlation with hsa_circ_0088196 in circRNA-associated ceRNA network.
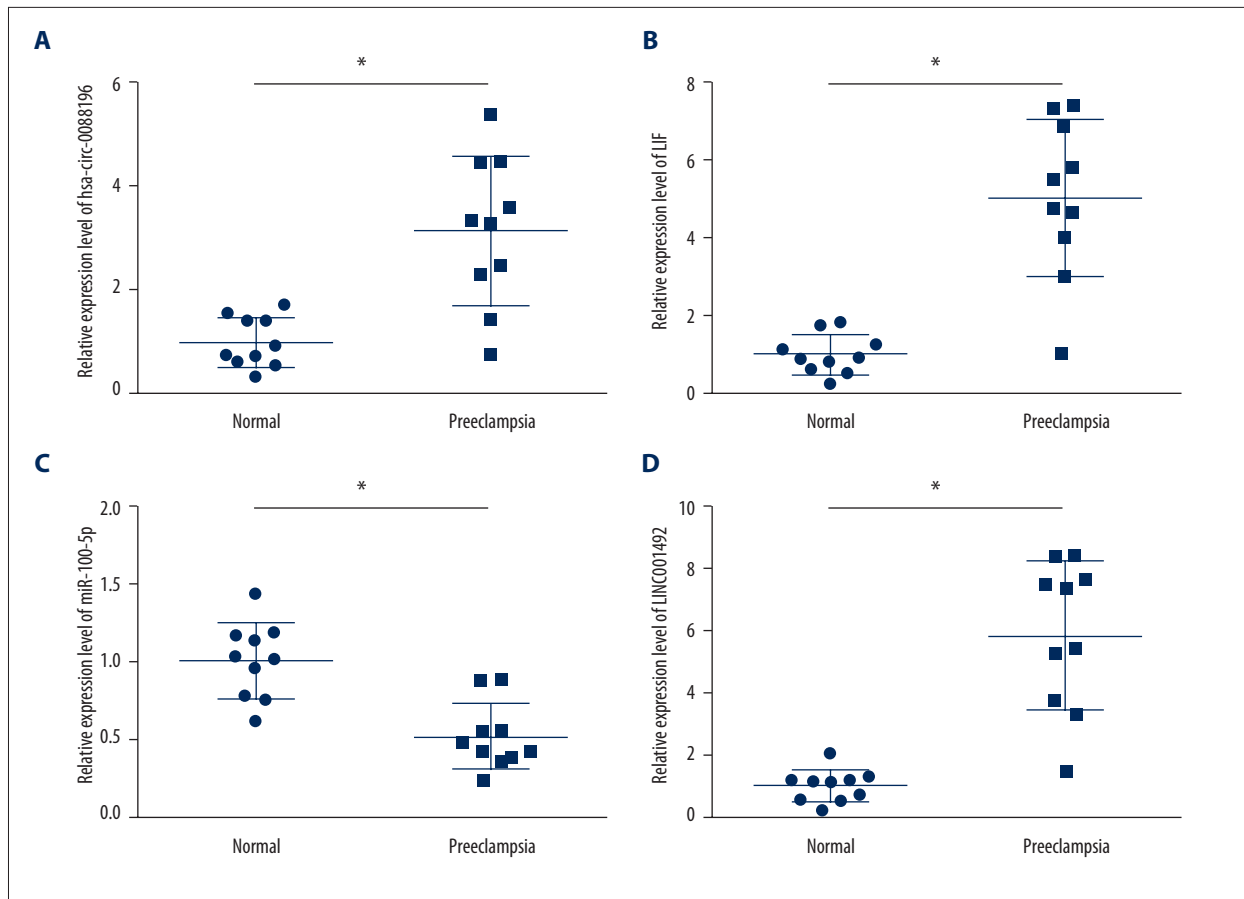
Figure 5. The expression levels of LIF, miR-100-5p, LINC01492, and hsa_circ_0088196 were investigated. (**A**) The expression levels of hsa_circ_0088196 in placental tissue, which is upregulated in PE. (**B**) The expression levels of LIF in placental tissue, which is upregulated in PE. (**C**) The expression levels of miR-100-5p in placental tissue, which is downregulated in PE. (**D**) The expression levels of LINC01492 in placental tissue, which is upregulated in PE. * $P<0.05$, compared with Normal group.

extracellular space (GO: 0005615) in CC was upregulated, which could be validated by Bubble plot. Through GSEA results which were visualized by ClusterProfiler and ggplot2 packages, we selected the jak-stat signaling pathway which was significantly activated in PE as our research subject. Through the ceRNA network, Venn diagram and target relationship prediction, we finally discovered the potentially meaningful in placental samples from PE patients. In addition, we verified the expression of mRNA LIF, miR-100-5p, LINC01492, and has_circ_0088196 expression in 10 paired placental samples from PE patients. As a result, miR-100-5p was lowly expressed and targeted by the 3'-UTR of LINC01492 and hsa_circ_0088196 and target the 3'-UTR of mRNA *LIF*, which were highly expressed.

Jak-stat signaling pathway was activated in this research, and the previous research has supplied similar solid evidence. Researchers have studied the effect of hypoxic preconditioning on the jak-stat 3 signaling pathway in PE and found that the expression levels of *jak* and *stat3* were much higher in the placental tissues of PE patients than in those of normal

pregnant women [27]. Moreover, some studies showed that some factors could work through jak-stat pathways. Malik et al. reported that epidermal growth factor (EGF) was low in PE and jak-stat pathway was involved in the process of EGF-mediated HTR-8/SVneo cell invasion [28]. Yin et al. showed that jak-stat pathways mediated the effect of IL-27 on the proinflammatory activation of PE [29]. In our study, we found that jak-stat signaling pathway was activated in PE. We also found that LIF was upregulated. Reports have shown that LIF could activated jak-stat 3 as a master regulator for the achievement and maintenance of naïve-state pluripotency [30]. Existing studies and our results suggest that it is important to study jak-stat pathways in PE.

Evidence showed that miR-100-5p played an important role in the development of PE. Hromadnikova et al. reported miR-100-5p was downregulated in placental tissues affected with PE [31]. Later, they reported the downregulation of miR-100-5p in maternal whole peripheral blood was a common phenomenon shared between gestational hypertension, PE, and
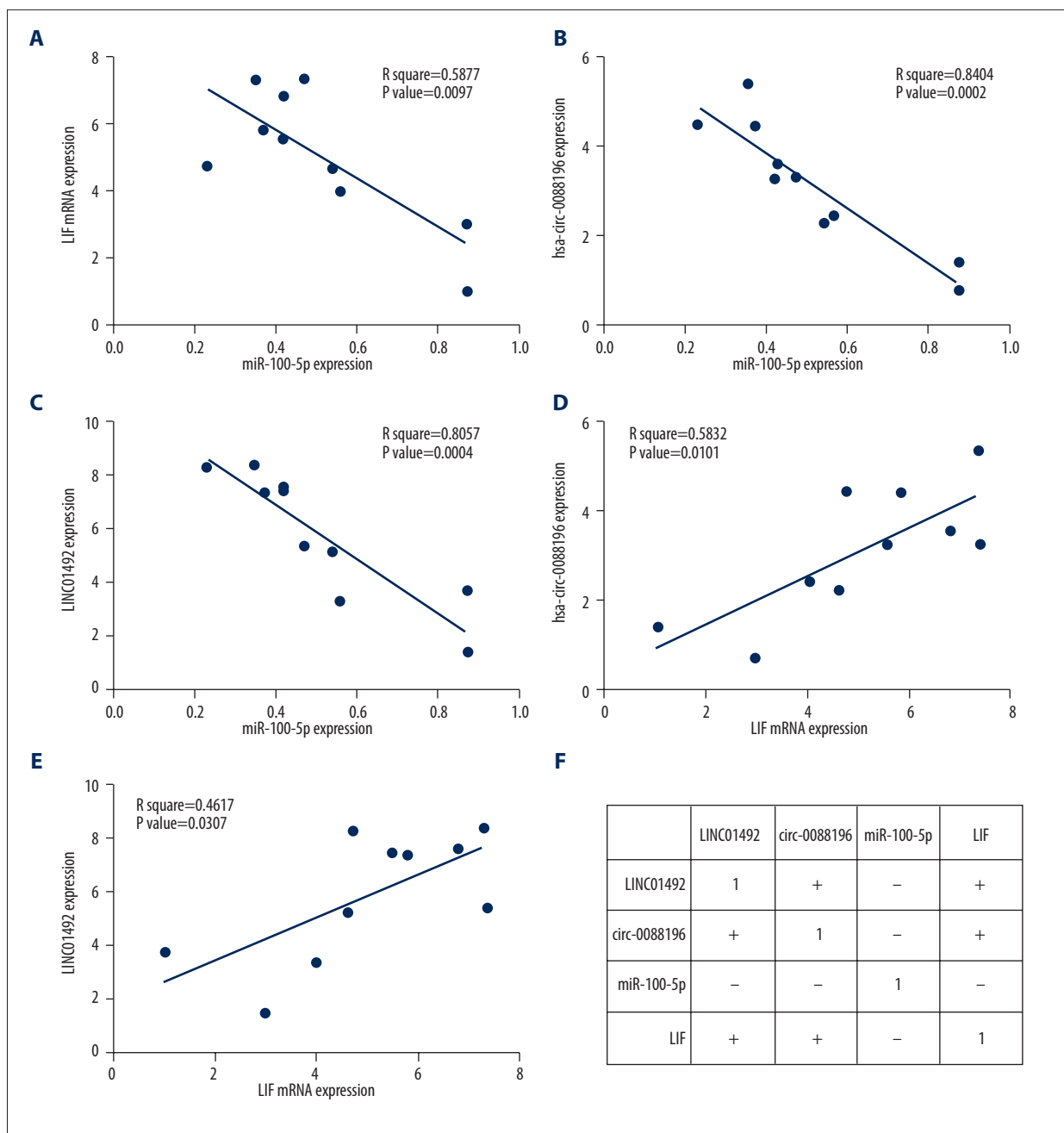
Figure 6. The correlations of LIF, miR-100-5p, LINC01492, and hsa_circ_0088196 expression levels. (**A**) miR-100-5p had negative correlation with LIF. (**B**) miR-100-5p had negative correlation with hsa_circ_0088196. (**C**) miR-100-5p had negative correlation with LINC01492. (**D**) LIF had positive correlation with hsa_circ_0088196. (**E**) LIF had positive correlation with LINC01492. (**F**) A table illustrating the expression level correlation of the 4 RNAs was placed, in which one indicates the same molecule, + indicates positive correlation and − indicates negative correlation.

intrauterine growth restriction [32]. Other studies showed that miR-100-5p was associated with many diseases. MiR-100-5p impacts the viability, migration, and apoptosis of cells in renal cell carcinoma [33]. Woo et al. found that miR-100-5p was downregulated in young women with attenuated ovarian reserve [34]. Yang et al. reported that miR-100-5p might be

related in recurrent miscarriage and might serve as a potential marker for recurrent miscarriage [35]. These results indicate that miR-100-5p is important for diagnosis and treatment of diseases. In our study, we found that miR-100-5p was down-regulated in PE. Therefore, further study is needed to identify
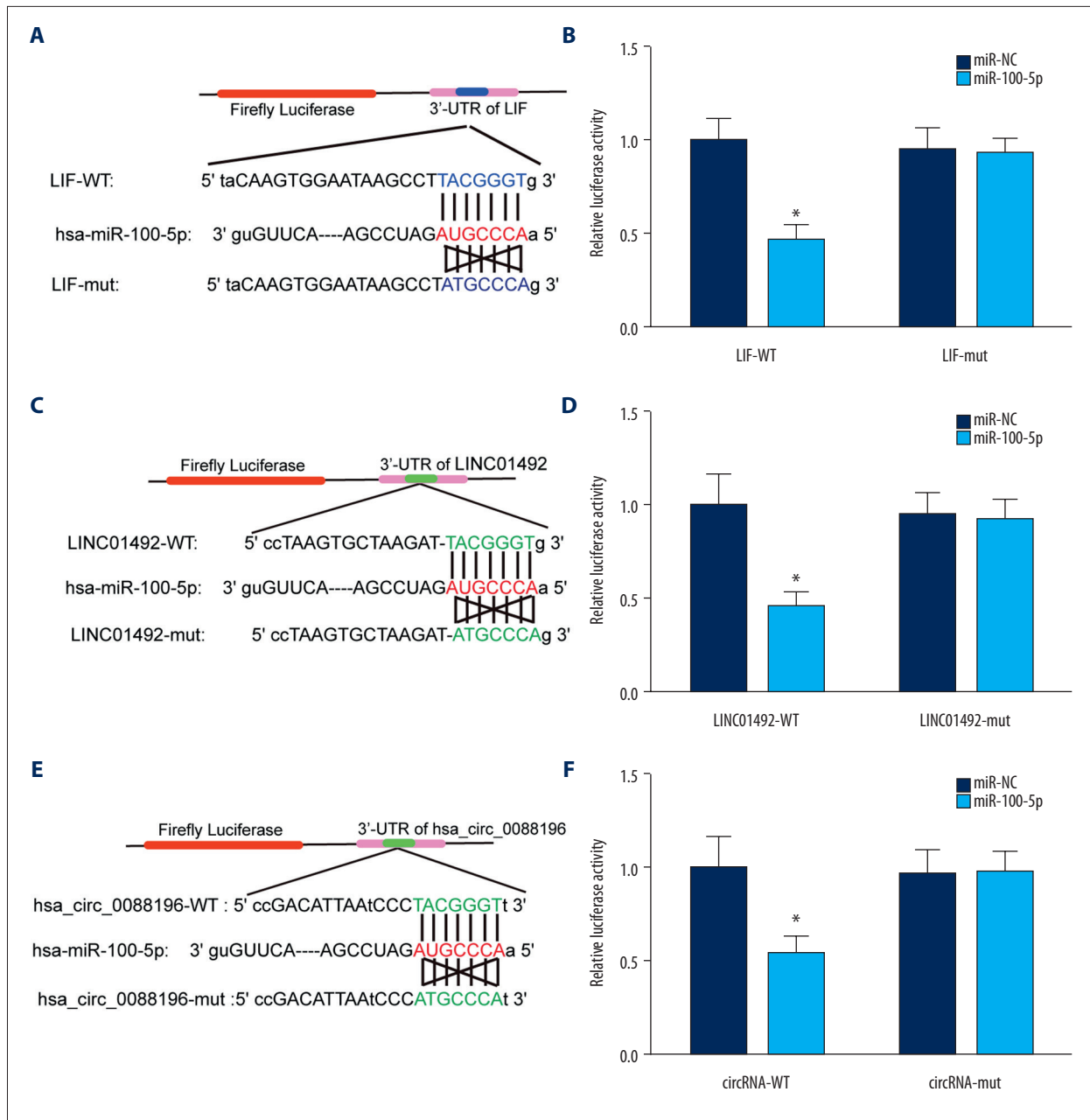
Figure 7. Targeting relationship verified by luciferase report assay. (**A**) Binding sites of LIF 3'-UTR targeted by miR-100-5p. (**B**) Wildtype binding site sequences of LIF co-transfected with miR-100-5p led to decreased luciferase activity, verifying their targeting relationship. (**C**) Binding sites of LINC01492 targeting miR-100-5p. (**D**) Wildtype binding site sequences of LINC01492 co-transfected with miR-100-5p led to decreased luciferase activity, verifying their targeting relationship. (**E**) Binding sites of hsa_circ_0088196 targeting miR-100-5p. (**F**) Wildtype binding site sequences of hsa_circ_0088196 co-transfected with miR-100-5p led to decreased luciferase activity, verifying their targeting relationship.

how miR-100-5p affects PE development. Our findings provide a theoretical basis for follow-up studies.

The mRNA LIF was selected through the jak-stat signaling pathway and ceRNA network in our research. Charkiewicz et al. reported a statistically significant increase in the concentration of

LIF in the plasma of women with PE [13]. The study launched by Zheng et al. indicated a role for LIF in promoting trophoblast migration and invasion through uPAR and suggested it might be associated with the etiology of PE [36]. Simultaneously, several studies found that LIF could be regulated by miRNA resulting in functional inhibition. Dong et al. found that miR-223-3p

inhibits LIF protein expression, which could lead to diminished embryo implantation [37]. In menstrual endometria and early pregnancy decidua, LIF was targeted by miR-423 which affects decidualization and the maintenance of early pregnancy [38]. Our study proved the upregulating of LIF in PE and predicted that miR-100-5p targeted LIF. These all revealed that LIF and miR-100-5p are important in the development of PE. It is necessary to ascertain role of LIF and miR-100-5p in PE.

In our analysis, hsa_circ_0088196 was found to be negatively associated with miR-500-5p and targeting miR-100-5p. Several studies had applied circRNAs as potential biomarkers for PE. Xu et al. collected a large quantity of samples and discovered that the level of circ_101222 was obviously higher in women with PE than that in normal women [21]. Chinese researchers conducted a comprehensive experiment that showed the relationship between PE and circRNAs, and they found that the area under the ROC curve for potential circRNAs, hsa_circRNA_100782, hsa_circRNA_102682, and hsa_circRNA_104820 were 0.653, 0.774 and 0.995 respectively, proving the potential significance of these circRNAs [20]. Briefly speaking, more efforts should be made toward the exploration of the differential expressions of circRNAs in PE.

For the upregulated lncRNA, we first found that the expression of LINC01492 was upregulated in PE. LINC01492 was negatively related with miR-100-5p. In fact, effects of lncRNAs in PE have been studied by many scholars. A group of research facilities in China opened the door to the determination the lncRNAs expression patterns in PE placenta using microarrays. The mechanisms underlying PE might be caused by the dysregulation of LOC284100, LOC391533, and CEACAMP8 [22]. The lncRNAs AF085938 and NR_027457 were found to be upregulated significantly, while AK002210 and G36948 were downregulated in PE, and all of them had vital diagnostic values for the PE detection [39]. Overall, more studies focused on differential lncRNAs in PE, will result I more effective treatments found for PE.

Conclusions

The jak-stat signaling pathway was chosen by GSEA analysis, and the upregulation of LIF, LINC01492, and hsa_circ_0088196 might promote PE by inhibiting miR-100-5p. More in-depth study about differentially expressed RNAs should be conducted to provide additional information about the future of PE treatment. Studies using blood serum samples should also be considered to confirm the conclusions of this study.

Conflict of interest

None.

References:

1. Guo L, Tsai SQ, Hardison NE et al: Differentially expressed microRNAs and affected biological pathways revealed by modulated modularity clustering (MMC) analysis of human preeclamptic and IUGR placentas. Placenta, 2013; 34: 599–605

2. Bai Y, Rao H, Chen W et al: Profiles of circular RNAs in human placenta and their potential roles related to preeclampsia. Biol Reprod, 2018; 98: 705–12

3. Ching T, Song MA, Tiirikainen M et al: Genome-wide hypermethylation coupled with promoter hypomethylation in the chorioamniotic membranes of early onset pre-eclampsia. Mol Hum Reprod, 2014; 20: 885–904

4. Song J, Li Y, An RF: Identification of early-onset preeclampsia-related genes and microRNAs by bioinformatics approaches. Reprod Sci, 2015; 22: 954–63

5. Zhao G, Zhou X, Chen S et al: Differential expression of microRNAs in decidua-derived mesenchymal stem cells from patients with pre-eclampsia. J Biomed Sci, 2014; 21: 81

6. Griffin JL, Atherton H, Shockcor J, Atzori L: Metabolomics as a tool for cardiac research. Nat Rev Cardiol, 2011; 8: 630–43

7. Sitras V, Fenton C, Acharya G: Gene expression profile in cardiovascular disease and preeclampsia: a meta-analysis of the transcriptome based on raw data from human studies deposited in Gene Expression Omnibus. Placenta, 2015; 36: 170–78

8. Bateman AR, El-Hachem N, Beck AH et al: Importance of collection in gene set enrichment analysis of drug response in cancer cell lines. Sci Rep, 2014; 4: 4092

9. Kanehisa M, Goto S: KEGG: kyoto encyclopedia of genes and genomes. Nucleic Acids Res, 2000; 28: 27–30

10. Biros E, Moran CS, Rush CM et al: Differential gene expression in the proximal neck of human abdominal aortic aneurysm. Atherosclerosis, 2014; 233: 211–18

11. Yu H, Yue X, Zhao Y et al: LIF negatively regulates tumour-suppressor p53 through Stat3/ID1/MDM2 in colorectal cancers. Nat Commun, 2014; 5: 5218

12. Cherepkova MY, Sineva GS, Pospelov VA: Leukemia inhibitory factor (LIF) withdrawal activates mTOR signaling pathway in mouse embryonic stem cells through the MEK/ERK/TSC2 pathway. Cell Death Dis, 2016; 7: e2050

13. Charkiewicz K, Jasinska E, Goscik J et al: Angiogenic factor screening in women with mild preeclampsia – new and significant proteins in plasma. Cytokine, 2018; 106: 125–30

14. Benian A, Uzun H, Aydin S et al: Placental stem cell markers in pre-eclampsia. Int J Gynaecol Obstet, 2008; 100: 228–33

15. Reister F, Kingdom JC, Ruck P et al: Altered protease expression by periarterial trophoblast cells in severe early-onset preeclampsia with IUGR. J Perinat Med, 2006; 34: 272–79

16. Van Sinderen M, Cuman C, Winship A et al: The chrondroitin sulfate proteoglycan (CSPG4) regulates human trophoblast function. Placenta, 2013; 34: 907–12

17. Chatterjee P, Weaver LE, Doersch KM et al: Placental Toll-like receptor 3 and Toll-like receptor 7/8 activation contributes to preeclampsia in humans and mice. PLoS One, 2012; 7: e41884

18. Ospina-Prieto S, Chaiwangyen W, Herrmann J et al: MicroRNA-141 is upregulated in preeclamptic placentae and regulates trophoblast invasion and intercellular communication. Transl Res, 2016; 172: 61–72

19. Biro O, Nagy B, Rigo J Jr.: Identifying miRNA regulatory mechanisms in preeclampsia by systems biology approaches. Hypertens Pregnancy, 2017; 36: 90–99

20. Qian Y, Lu Y, Rui C et al: Potential significance of circular RNA in human placental tissue for patients with preeclampsia. Cell Physiol Biochem, 2016; 39: 1380–90

21. Zhang YG, Yang HL, Long Y, Li WL: Circular RNA in blood corpuscles combined with plasma protein factor for early prediction of pre-eclampsia. BJOG, 2016; 123: 2113–18

22. He X, He Y, Xi B et al: LncRNAs expression in preeclampsia placenta reveals the potential role of LncRNAs contributing to preeclampsia pathogenesis. PLoS One, 2013; 8: e81437

23. Chen H, Meng T, Liu X et al: Long non-coding RNA MALAT-1 is downregulated in preeclampsia and regulates proliferation, apoptosis, migration and invasion of JEG-3 trophoblast cells. Int J Clin Exp Pathol, 2015; 8: 12718–27

24. Cox B, Leavey K, Nosi U et al: Placental transcriptome in development and pathology: Expression, function, and methods of analysis. Am J Obstet Gynecol, 2015; 213: S138–51

25. Yang HB, Jiang J, Li LL et al: Biomarker identification of thyroid associated ophthalmopathy using microarray data. Int J Ophthalmol, 2018; 11: 1482–88

26. Mukaka MM: Statistics corner: A guide to appropriate use of correlation coefficient in medical research. Malawi Med J, 2012; 24: 69–71

27. Xu C, Li X, Guo P, Wang J: Hypoxia-induced activation of jak/stat3 signaling pathway promotes trophoblast cell viability and angiogenesis in preeclampsia. Med Sci Monit, 2017; 23: 4909–17

28. Malik A, Pal R, Gupta SK: Interdependence of JAK-STAT and MAPK signaling pathways during EGF-mediated HTR-8/SVneo cell invasion. PLoS One, 2017; 12: e0178269

29. Yin N, Zhang H, Luo X et al: IL-27 activates human trophoblasts to express IP-10 and IL-6: Implications in the immunopathophysiology of preeclampsia. Mediators Inflamm, 2014; 2014: 926875

30. Huang D, Wang L, Duan J et al: LIF-activated Jak signaling determines Esrrb expression during late-stage reprogramming. Biol Open 2018; 7(1): pii: bio029264

31. Hromadnikova I, Kotlabova K, Hympanova L, Krofta L: Cardiovascular and cerebrovascular disease associated microRNAs are dysregulated in placental tissues affected with gestational hypertension, preeclampsia and intrauterine growth restriction. PLoS One, 2015; 10: e0138383

32. Hromadnikova I, Kotlabova K, Hympanova L, Krofta L: Gestational hypertension, preeclampsia and intrauterine growth restriction induce dysregulation of cardiovascular and cerebrovascular disease associated microRNAs in maternal whole peripheral blood. Thromb Res, 2016; 137: 126–40

33. Chen P, Lin C, Quan J et al: Oncogenic miR-100-5p is associated with cellular viability, migration and apoptosis in renal cell carcinoma. Mol Med Rep, 2017; 16: 5023–30

34. Woo I, Christenson LK, Gunewardena S et al: Micro-RNAs involved in cellular proliferation have altered expression profiles in granulosa of young women with diminished ovarian reserve. J Assist Reprod Genet, 2018; 35(10): 1777–86

35. Yang Q, Gu WW, Gu Y et al: Association of the peripheral blood levels of circulating microRNAs with both recurrent miscarriage and the outcomes of embryo transfer in an in vitro fertilization process. J Transl Med, 2018; 16: 186

36. Zheng Q, Dai K, Cui X et al: Leukemia inhibitory factor promote trophoblast invasion via urokinase-type plasminogen activator receptor in preeclampsia. Biomed Pharmacother, 2016; 80: 102–8

37. Dong X, Sui C, Huang K et al: MicroRNA-223-3p suppresses leukemia inhibitory factor expression and pinopodes formation during embryo implantation in mice. Am J Transl Res, 2016; 8: 1155–63

38. Lv Y, Gao S, Zhang Y et al: miRNA and target gene expression in menstrual endometria and early pregnancy decidua. Eur J Obstet Gynecol Reprod Biol, 2016; 197: 27–30

39. Luo X, Li X: Long non-coding RNAs serve as diagnostic biomarkers of preeclampsia and modulate migration and invasiveness of trophoblast cells. Med Sci Monit, 2018; 24: 84–91